Comparison of Mode-Matching and Differential Equation Techniques in the Analysis of Waveguide Transitions

William A. Huting, *Member, IEEE*, and Kevin J. Webb, *Member, IEEE*

Abstract—**The solution of the continuous waveguide transition problem can be obtained by discretizing the boundary and applying mode matching or by using a system of ordinary differential equations. Both approaches involve approximate representations of the boundary. When using the differential equation approach, it was found necessary to consider the transition as several sections in series in order to avoid numerical instabilities. When this is done, one may cascade using a generalized scattering matrix approach or a generalized *ABCD* matrix method. Results are shown comparing the accuracy of the boundary discretization approach and the differential equation approach for the Marie transducer and for linear transitions of various lengths in rectangular waveguide. Experimental results are also given for the Marie transducer.**

I. Introduction

NUMERICAL approaches to the continuous waveguide transition analysis and design problems have been studied for the past 20 or so years (e.g., [1]–[5]). Recently, the authors used a novel moment method technique to solve a system of ordinary differential equations describing such a transition [4], [5]. The present paper, which is basically an extension of the work in [4] and [5], includes a comparison of the differential equation method with an approach which approximates the transition as a series of discrete steps and subsequently applies mode matching, an application of these techniques to linear rectangular transitions, a discussion of the validity of the differential equations and associated boundary conditions, and experimental and numerical results for the Marie rectangular TE_{10} to circular TE_{01} mode transducer. Also included are new results regarding the sensitivity of the computed solution to the choice of cascading formulation when, as is a fairly common practice [3]–[5], a transition is analyzed as several sections in series in order to avoid numerical instabilities.

II. Methods of Solution

The system of differential equations used in this paper is based on the assumption that the transverse portion of the electromagnetic field in a transition can be written as a sum of the uniform waveguide mode functions corresponding to the local transition cross section:

$$\boldsymbol{E}_t(x,y,z) = \sum_{m=1}^{\infty} V_m(z)\boldsymbol{e}_m(x,y,z) \tag{1}$$

$$\boldsymbol{H}_t(x,y,z) = \sum_{m=1}^{\infty} I_m(z)\boldsymbol{h}_m(x,y,z) \tag{2}$$

where z denotes the direction of propagation, and the parameters $V_m(z)$ and $I_m(z)$ are known respectively as the equivalent voltages and the equivalent currents. A system of ordinary differential equations which specifies $V_m(z)$ and $I_m(z)$ was given by Reiter in 1959 [6] and methods of solution are discussed at some length in [3]–[5]. These equations are

$$\frac{dV_m}{dz} = -j\beta_m Z_m I_m + \sum_{n=1}^{\infty} T_{mn}V_n \tag{3}$$

$$\frac{dI_m}{dz} = -j\frac{\beta_m}{Z_m}V_m - \sum_{n=1}^{\infty} T_{nm}I_n. \tag{4}$$

Both TE and TM modes are included in (3) and (4). The variable β_m denotes the wavenumber of the mth mode, the variable Z_m denotes the wave impedance of the mth mode, and the "transfer coefficients" T_{mn} (which describe coupling between the two modes m and n) are given by [6]

$$T_{mn}(z) = \iint_{S(z)} \frac{d\boldsymbol{e}_m}{dz}\cdot\boldsymbol{e}_n\,dx\,dy. \tag{5}$$

The integration in (5) is over the local waveguide cross section, $S(z)$. If the system of equations in (3) and (4) is truncated and then solved for the portion of the transition between $z = z_t$ and $z = z_{t+1}$, one may specify numerical values for the associated generalized *ABCD* matrix:

$$\begin{bmatrix} V(z_{t+1}) \\ I(z_{t+1}) \end{bmatrix} = \begin{bmatrix} A_t & B_t \\ C_t & D_t \end{bmatrix}\begin{bmatrix} V(z_t) \\ I(z_t) \end{bmatrix} \tag{6}$$

where the dimension of the square submatrices A_t, B_t, C_t, and D_t is equal to the number of modes (propagating and evanescent) included in the solution. Cascading the results for two adjacent portions of the transition may be accomplished by simple multiplication of the two *ABCD* matrices [4], [5] or by translating these two matrices into generalized scattering matrices and then linking them together [3]. One goal of this paper is to compare the efficacy of these two

Manuscript received March 12, 1990; revised August 15, 1990.

W. A. Huting is with the Applied Physics Laboratory, Johns Hopkins University, Laurel, MD 20723.

K. J. Webb was with the Electrical Engineering Department, University of Maryland, College Park. He is now with the School of Electrical Engineering, Purdue University, West Lafayette, IN 47907.

IEEE Log Number 9041462.

0018-9480/91/0200-0280$01.00 ©1991 IEEE

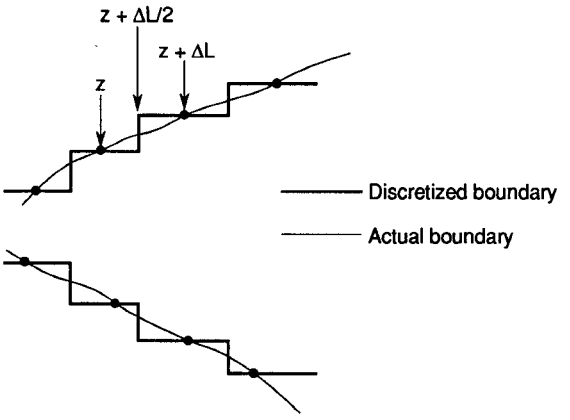

Fig. 1. Boundary discretization geometry.

cascading approaches. The *ABCD* matrix approach is computationally less intensive, and therefore initially more attractive, than the scattering matrix approach.

One well-known alternative to solving the differential equations is to discretize the boundary and to apply mode matching. The boundary discretization geometry used in this paper is depicted in Fig. 1. The two uniform waveguides in this figure have cross sections equivalent to the transition cross sections at z and $z + \Delta L$. As shown in [7], the difference equation for the equivalent voltages and currents is

$$\begin{aligned} V_m(z+\Delta L) &= \cos\left(\frac{\beta_m \Delta L}{2}\right) \sum_{n=1}^{\infty} \cos\left(\frac{\beta_n \Delta L}{2}\right) \\ &\quad \cdot \left(\iint_S e_n(z) \cdot e_m(z+\Delta L)\, dx\, dy \right) V_n(z) \\ &\quad - \cos\left(\frac{\beta_m \Delta L}{2}\right) \sum_{n=1}^{\infty} jZ_n(z) \sin\left(\frac{\beta_n \Delta L}{2}\right) \\ &\quad \cdot \left(\iint_S e_n(z) \cdot e_m(z+\Delta L)\, dx\, dy \right) I_n(z) \\ &\quad + jZ_m(z+\Delta L) \sin\left(\frac{\beta_m \Delta L}{2}\right) \\ &\quad \cdot \sum_{n=1}^{\infty} \frac{j}{Z_n(z)} \sin\left(\frac{\beta_n \Delta L}{2}\right) \\ &\quad \cdot \left(\iint_S e_n(z) \cdot e_m(z+\Delta L)\, dx\, dy \right) V_n(z) \\ &\quad - jZ_m(z+\Delta L) \sin\left(\frac{\beta_m \Delta L}{2}\right) \cdot \\ &\quad \cdot \sum_{n=1}^{\infty} \cos\left(\frac{\beta_n \Delta L}{2}\right) \\ &\quad \cdot \left(\iint_S e_n(z) \cdot e_m(z+\Delta L)\, dx\, dy \right) I_n(z) \end{aligned} \tag{7}$$

where the area of integration, S, is equal to the intersection of $S(z)$ and $S(z + \Delta L)$. Rewriting (7) as a sum of powers of ΔL and retaining only terms of order $(\Delta L)^2$ or lower, one obtains

$$\begin{aligned} &V_m(z+\Delta L) \\ &\quad = V_m(z) - j\Delta L Z_m(z) \beta_m(z) I_m(z) \\ &\qquad + \Delta L \sum_{n=1}^{\infty} \left(\iint_S e_m'(z) \cdot e_n(z)\, dx\, dy \right) V_n(z) \\ &\qquad - (\Delta L)^2 \frac{(\beta_m(z))^2}{4} V_m(z) \\ &\qquad - j(\Delta L)^2 Z_m'(z) \frac{\beta_m(z)}{2} I_m(z) \\ &\qquad + \frac{(\Delta L)^2}{2} \sum_{n=1}^{\infty} \left(\iint_S e_m''(z) \cdot e_n(z)\, dx\, dy \right) V_n(z) \\ &\qquad - j(\Delta L)^2 \sum_{n=1}^{\infty} \left(Z_n(z) \frac{\beta_n(z)}{2} + Z_m(z) \frac{\beta_m(z)}{2} \right) \\ &\qquad \cdot \left(\iint_S e_m'(z) \cdot e_n(z)\, dx\, dy \right) I_n(z) \end{aligned} \tag{8}$$

where the primes refer to differentiation with respect to z. A similar equation exists for I_m. It is easily seen that, in the limit of vanishing ΔL, (8) reduces to (3). Therefore, one might expect that the boundary discretization method should converge to the same solution as does the differential equation method. However, convergence rates can be affected by the $(\Delta L)^2$ terms and these terms do, in fact, differ between (8) and some of the techniques for solving (3) and (4), e.g., the Runge–Kutta method [7]. Similar difference equations can be derived when traveling waves are considered instead of the equivalent voltages and currents of (1) and (2), and further details are given in [7]. The mode-matching approach used in this paper [8, ch. 5] is a modification of the method described by Carin, Webb, and Weinreb [9], and the scattering matrix cascading technique described by Chu and Itoh [10] is used to link together the large number of junctions used to approximate a transition.

Finally, it should be noted that although (3) and (8) indicate that the differential equation method and the boundary discretization method should converge to a common solution, the two methods are based on somewhat different representations of the transition boundary. The differential equation approach assumes a perfectly smooth boundary while the mode-matching approach uses a stepped boundary. It may not be correct to say that the stepped boundary is a valid approximation of the smooth boundary. This is well illustrated if one attempts to approximate the diagonal of a unit square as a series of steps: the approximate boundary will have a length equal to 2 independent of the number of steps whereas the actual diagonal has a length equal to $\sqrt{2}$. Nonetheless, in spite of these two rather different boundary representations, (3) and (8) appear to indicate that the two methods are equivalent. This can perhaps be explained as follows. Most standard methods for solving (3) can be written as difference equations similar to (8). Any difference equation approach for solving (3) will include terms of $(\Delta L)^2$ and higher, and for nonzero ΔL, these higher order terms will represent a distortion of the smooth system of (3). This distortion vanishes as ΔL vanishes, result-

ing in the equivalence of (3) and (8). Yet another interesting issue is whether or not (1) and (2) are appropriate for nonuniform waveguides. This will be discussed at the end of Section IV.

III. Marie Transducer Analysis

In this section, the numerical techniques described above are applied to an X-band model of the Marie rectangular TE_{10} to circular TE_{01} mode transducer [11] and the resultant data are compared with experimental results. This device, which has been informally described as "the best transition to TE_{01}" [12], is shown in Fig. 2 and the desired electric field lines at various locations are shown in Fig. 3. (The circular taper portion in Fig. 2 is not included in some models.)

A detailed study of the Marie transducer was performed by Saad, Davies, and Davies in the 1970's [1], [2], [13]. One difference between their work and ours is that they numerically implemented Solymar's small coupling procedure [14], while we use the methods described in [4] and [5]. A prerequisite for analyzing a continuous waveguide transition is to obtain the mode functions in (1) and (2). These modal solutions and the associated eigenvalues are essential in determining the coefficients in Reiter's equations [4], [6]. As noted in [13], these tasks must be accomplished numerically when one considers an irregularly shaped device such as the Marie transducer. The publicly available software we used is described in [15] and [16], and further details regarding our particular implementation can be found in [8]. In the circular taper portion of the transition, the coefficients for the differential equations may be determined analytically [17].

The generation of numerical data describing the transmission and reflection properties of this device will now be described. These data will be compared with measurements performed on two Marie transducers connected to each other by a 35 in. long metallic circular waveguide, i.e., launching and detecting at the two rectangular ports. Each Marie transducer was 46.35 in. long with circular taper portions each 11 in. long. The circular ends of the Marie transducer were 1.18 in. in radius and the rectangular ends were standard WR-90 waveguide. The numerical data were acquired using four schemes:

Approach 1: In the irregularly shaped portions of the Marie transducer, only the desired rectangular TE_{10}–circular TE_{01} mode is included in the expansions (1) and (2), and in the most narrow part of the circular taper, only the desired TE_{01} mode was considered. Only a single mode was considered because previous work [4] indicates that considering only modes near or above cutoff is sufficiently accurate while reducing computational complexity. All of these "one-mode" sections were analyzed using the Runge–Kutta technique to solve the truncated system of differential equations [4]. In a middle 1 in. portion of the taper, where the unwanted TE_{02} mode goes through cutoff, both this mode and the TE_{01} mode were included and the moment method of [4] was used. The reason for selecting this technique is that, as observed in [3] and [4], evanescent modes cause numerical problems, and the results of [4] seem to indicate that the moment method technique has better stability characteristics than do some conventional techniques (e.g., the Runge–Kutta method and an iterative integration technique [4], [5]). Finally, in the widest part of the taper, where both modes were above cutoff, the numerically less expensive Runge–Kutta

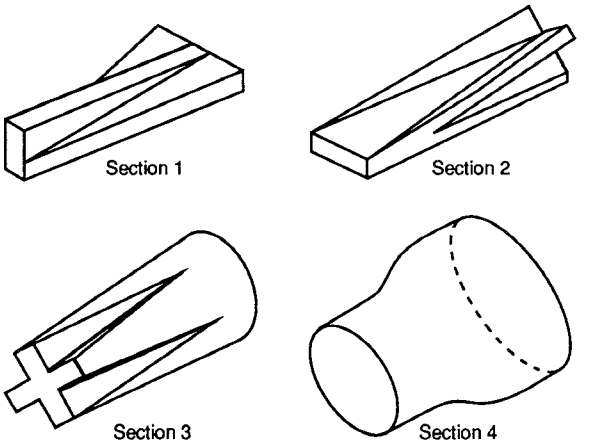

Fig. 2. The Marie transducer.

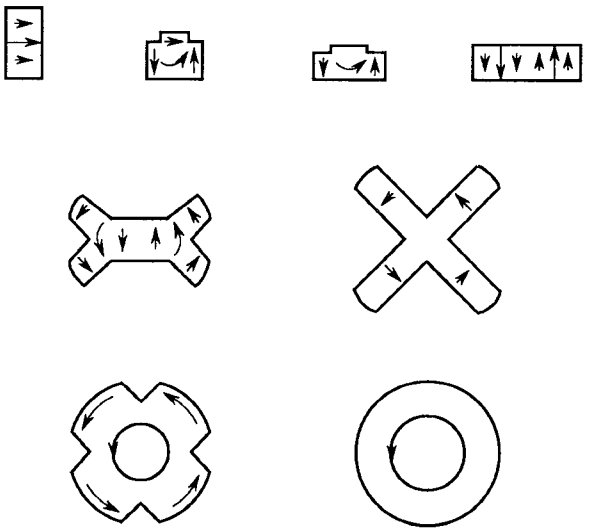

Fig. 3. Desired electric field lines for the Marie transducer.

technique was used. As in [4], cascading was accomplished through the simple multiplication of the generalized *ABCD* matrices representing adjacent cross sections. First, the 4×4 TE_{01}–TE_{02} *ABCD* matrices representing the circular waveguide and the wider portions of the circular tapers of the two Marie transducers were combined to produce a 4×4 *ABCD* matrix. The four elements of this matrix which describe TE_{01} to TE_{01} interaction were used to produce a 2×2 *ABCD* matrix which was then cascaded with the "single-mode" sections. This new 2×2 matrix was then translated into a 2×2 scattering matrix. For further details, see [8, ch. 4].

In order to verify these calculations, measurements were performed using a Wiltron 360 network analyzer between 11 and 12 GHz. These tests included a calibration procedure which allowed normalization of the test data in the presence of imperfect connections, cables, etc., between the unit under test and the network analyzer input and output ports. (To further establish the validity of these tests, all measurements were repeated several times and tests were performed on known devices. We believe that the $|S_{21}|$ data are accurate to within ±0.1 dB and $|S_{11}|$ to within ±10.0 dB. For further details, see [7].) Fig. 4 shows numerical and experimental data for the scattering parameter S_{21} for the two Marie

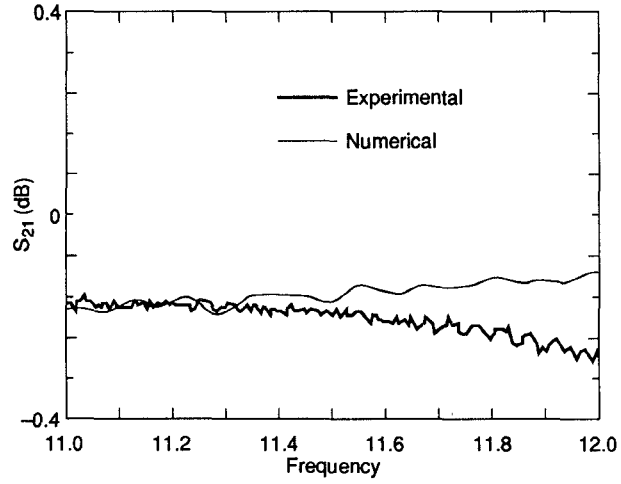

Fig. 4. Experimental and numerical $|S_{21}|$ for system consisting of two Marie transducers connected by a circular waveguide. These data were generated using the *ABCD* matrix cascading formulation (approach 1 in text).

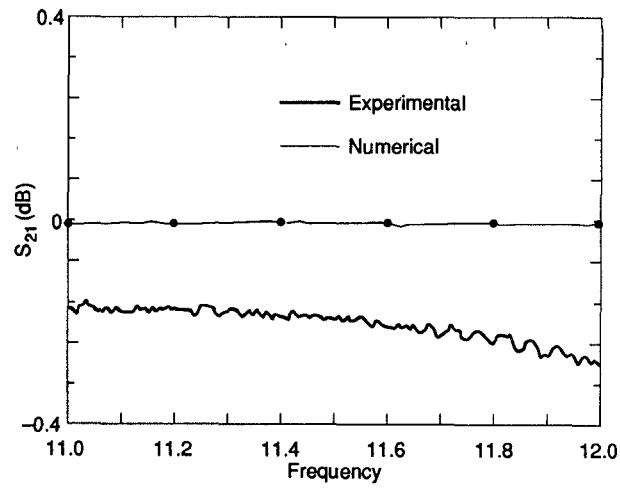

Fig. 6. Experimental and numerical $|S_{21}|$ for system consisting of two Marie transducers connected by a circular waveguide. These data were generated using the scattering matrix cascading formulation (thin line: approaches 2, 3 in text; dots: approach 4 in text).

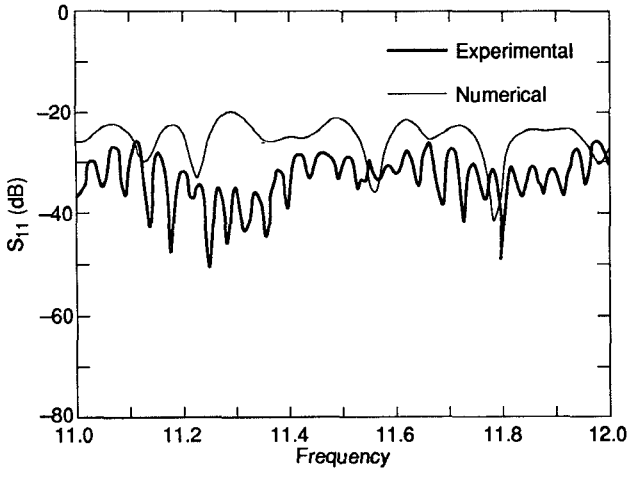

Fig. 5. Experimental and numerical $|S_{11}|$ for system consisting of two Marie transducers connected by a circular waveguide. These data were generated using the *ABCD* matrix cascading formulation (approach 1 in text).

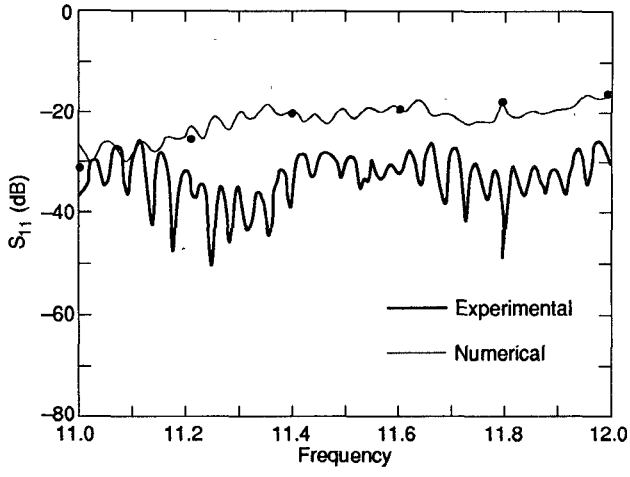

Fig. 7. Experimental and numerical $|S_{11}|$ for system consisting of two Marie transducers connected by a circular waveguide. These data were generated using the scattering matrix cascading formulation (thin line: approaches 2, 3 in text; dots: approach 4 in text).

transducers and the connecting circular waveguide. Fig. 5 shows the results for S_{11}. The experimental data indicate very low but observable dissipative loss.

Approach 2: The second method of analysis differed from approach 1 in only one respect: cascading. The individual 4×4 *ABCD* matrices were converted into 4×4 scattering matrices *before* cascading. Chu and Itoh have published a method for cascading two devices represented by generalized scattering matrices and connected by a uniform waveguide [10]. In cascading two adjacent portions of the transition, this method was used with the length of the uniform waveguide set equal to zero in the computer program. Once the "two-mode" sections were cascaded, the four elements of the generalized scattering matrix representing TE_{01} to TE_{01} interaction were used to produce a 2×2 scattering matrix which was then cascaded with the "single-mode" sections. Cascading such 2×2 matrices is a trivial task, and was done according to [18, pp. 150–151]. Figs. 6 and 7 show the data generated using this approach along with the experimental data from Figs. 4 and 5.

Approach 3: The third approach differed from approach 2 in only one respect: the middle part of the circular taper was analyzed using boundary discretization and mode matching. Five modes were considered at five junctions and the resultant scattering matrix was converted into a two-mode scattering matrix (by simple truncation) before cascading with the other "two-mode" sections. Results obtained using this approach were identical to those of approach 2, i.e., Figs. 6 and 7.

Approach 4: Boundary discretization and mode matching were used to analyze the *entire* circular taper. *Nine* modes were used at each junction and the taper was approximated by 50 junctions. A 2×2 scattering matrix was extracted from the results and cascaded with the irregularly shaped "single-mode" sections. These results were very close to those of approaches 2 and 3, i.e., the thin lines in Figs. 6 and 7.

By examining Figs. 4–7, it is seen that, at least for this example, the computed solution is insensitive to whether the differential equation technique or the mode-matching technique is used. However, this is not true regarding the choice of cascading method. One might conclude that the *ABCD* matrix multiplication technique used in approach 1 provided a more accurate solution than the scattering matrix cascading technique used in the other three approaches because the numerical and experimental curves are more closely coincident in Figs. 4 and 5 than in Figs. 6 and 7. However, it should be noted that these calculations do not take conductive losses into account; a "good" solution would therefore show insertion losses slightly less than in the experiment. If observable losses are expected, the scattering matrix cascading data of Figs. 6 and 7 appear more credible than the approach 1 data of Figs. 4 and 5. Further, in this case the scattering matrix formulation involved manipulating 2×2 submatrices with condition numbers in the range 10^0 to 10^2, while the generalized *ABCD* matrix formulation involved manipulating 4×4 matrices with condition numbers of 10^5. To sum up, for this particular example, the scattering matrix formulation utilized smaller and better conditioned matrices and yielded physically more reasonable results than does the *ABCD* matrix formulation.

A comparison of computer times for the moment method program and the mode-matching program used in the above examples indicates no substantial advantage from the viewpoint of computational efficiency. A similar conclusion is reached when these programs are used to analyze a simple rectangular taper [8]. It should be noted that neither of these two programs has yet been optimized with respect to either run time or storage. The Runge–Kutta technique is by far the least expensive of the methods considered here, and, as indicated in [4], it is sufficiently accurate in many cases.

IV. Continuous Versus Discrete Formulations

In Section III, our particular implementations of the differential equation approach and the boundary discretization approach yielded virtually identical results when applied to the circular taper portion of a Marie transducer. This taper varies slowly with respect to wavelength. It also has been reported that the two approaches yield identical data for a slowly varying rectangular taper [8] and several extremely slowly varying circular tapers [3]. In this section, we show that the routines are also consistent for rapidly varying transitions. Our treatment starts with the rectangular taper of Fig. 8, with the taper length L as a parameter. This taper is analyzed for extremely short lengths L using the previously described techniques. The $L=0$ case, which is simply an abrupt discontinuity, is analyzed using a single-step mode-matching routine. (The differential equation technique clearly will not work for $L=0$.) The idea is to see whether or not, for diminishing lengths L, the waveguide transition data approach the abrupt discontinuity results and to compare the differential equation data with the boundary discretization data for these nonzero lengths L.

Fig. 8 shows a transition between two rectangular waveguides with different heights. For the dimensions given, we shall consider the band between 1.0 and 1.8 GHz, where only the TE_{10} mode is capable of propagation. The abrupt ($L=0$) case was analyzed using two methods, namely, a nine-mode mode-matching solution and a simple procedure which used

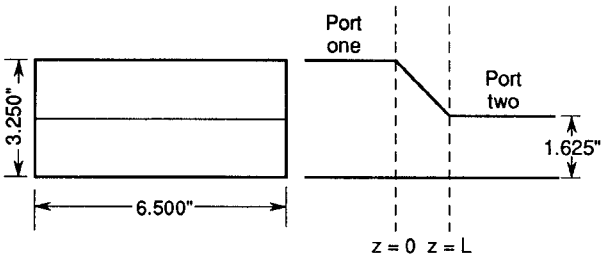

Fig. 8. Steep rectangular waveguide taper discussed in Section IV.

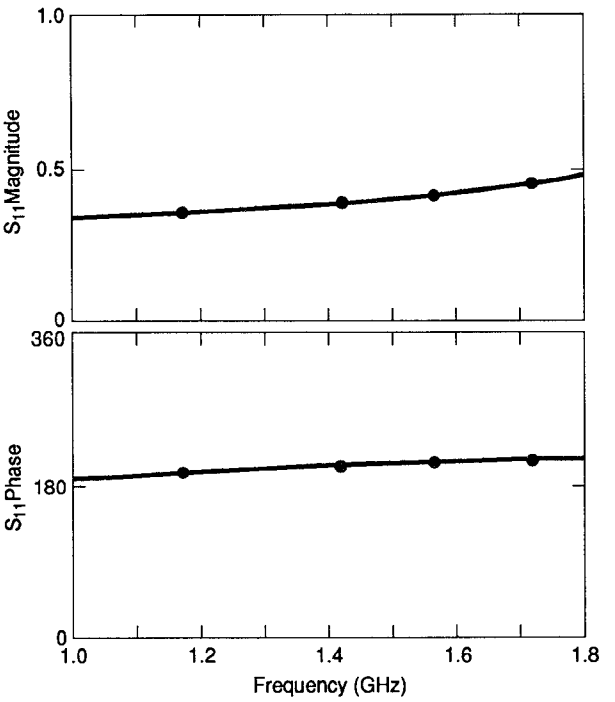

Fig. 9. Computed reflection coefficient for the steep taper of Fig. 7 for the abrupt discontinuity ($L=0$) case. The solid line was generated using mode matching with nine modes. The dots were generated using [19, fig. 5.26-3].

data from a figure in Marcuvitz's book [19, Fig. 5.26-3]. Fig. 9 shows the dominant mode reflection coefficient S_{11} obtained by these two methods, and the two sets of data are coincident. Subsequently, results were generated for the lengths $L=0.05\lambda_0$, $0.025\lambda_0$, $0.001\lambda_0$, and $10^{-9}\lambda_0$, where λ_0 is the free-space wavelength at 1.0 GHz. These results were generated taking into account the nine lowest modes and using two analytical techniques. First, boundary discretization and mode matching were applied with 100 junctions between $z=0$ and $z=L$. Second, the Galerkin method version of the moment method technique [4] was used with two cascaded sections between $z=0$ and $z=L$ and with five triangle weighting functions per section. For each length, the two sets of curves were indistinguishable, and these curves are shown in Fig. 10. The results for $L=10^{-9}\lambda_0$ are very close to the $L=0$ results of Fig. 9 generated using a nine-mode, single-step mode-matching routine.

For the above short transition example, the differential equation technique and the boundary discretization technique are in agreement, just as they were for gradual tapers. Indeed, consistency between these two methods is what one

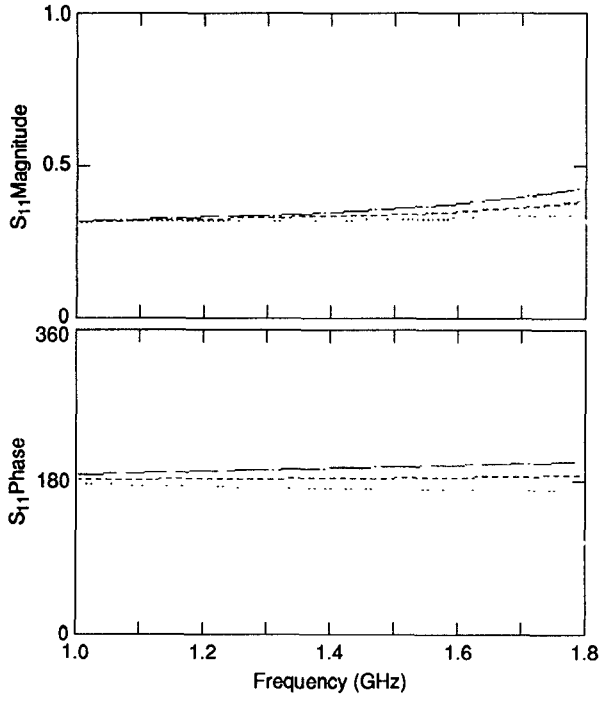

Fig. 10. Computed reflection coefficient for the steep taper of Fig. 7 for the cases $L = 0.05\lambda_0$ (dots), $L = 0.025\lambda_0$ (dash), $L = 0.001\lambda_0$ (chaindot), and $L = 10^{-9}\lambda_0$ (chaindot), where λ_0 is the free-space wavelength at 1.0 GHz. Each of these four sets of data was generated using the differential equation method and the boundary discretization method (nine modes). The two methods yielded identical results.

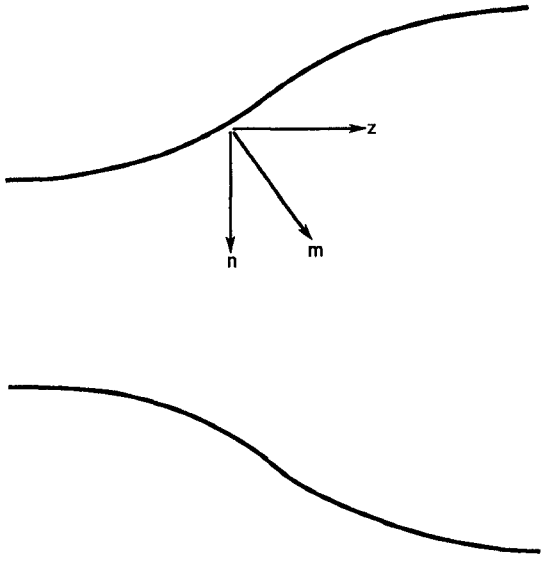

Fig. 11. Waveguide transition geometry for electromagnetic boundary conditions.

would expect after examining (3) and (8). We think this agreement between the two techniques might be theoretically important. This is because, as observed in [20], the magnetic field expansion (2) cannot satisfy the transition wall boundary condition exactly. At the wall, the magnetic field must satisfy (Fig. 11)

$$\boldsymbol{H}\cdot\boldsymbol{m} = 0. \tag{9}$$

The individual terms of the expansion satisfy

$$\boldsymbol{h}_m\cdot\boldsymbol{n} = 0. \tag{10}$$

(The boundary condition for the electric field is satisfied by the individual terms of (1).) If the transition is a slowly varying (i.e., nearly uniform) one, (9) and (10) are approximately the same, but for rapidly varying tapers, the unit vectors $\boldsymbol{m}$ and $\boldsymbol{n}$ become less coincident, the approximation breaks down, and one might question the validity of the differential equation method. However, for the steep taper in Fig. 8, the differential equation method yields the same results as the boundary discretization technique and these two identical sets of results converge to the abrupt discontinuity solution for diminishing values of L. Moreover, consistency among these same techniques when applied to a steep circular waveguide taper has also been reported [7]. Thus, the differential equation formulation appears to be suitable even for rapidly varying tapers. One possible explanation for this may be found in an idea advanced by Unger [20], namely, that the expansion (2) is valid, that it converges to the correct field values inside but not on the boundary, and that this expansion therefore suffers a discontinuity on the boundary. Recently, it has been argued that the mathematics of the derivation of Reiter's equations are fully consistent with the existence of an expansion with these attributes [8, pp. 3–17].

V. Conclusion

Several waveguide transitions have been analyzed using two different methods: (i) discretizing the transition boundary and using mode matching and (ii) solving a system of ordinary differential equations. For gradual transitions, the two methods lead to identical results and use comparable amounts of computer time (assuming the same number of modes are used in both cases). For extremely steep transitions (excluding the step transition), our results still indicate agreement between the two methods. Our results also indicate that the scattering matrix cascading method (previously used in [3]) leads to results which are more credible than those obtained when cascading is performed by multiplying generalized *ABCD* matrices. The differential equation technique may be more generally applicable for continuous transitions in that artificial discontinuities are not introduced and an arbitrary number (including zero) of evanescent modes can be introduced.

Acknowledgment

The authors are grateful to G. Vetticad for his assistance in obtaining the experimental data in Figs. 4–7.

References

[1] S. S. Saad, J. B. Davies, and O. J. Davies, "Analysis and design of a circular TE_{01} mode transducer," *IEE J. Microwaves, Opt. Acoust.*, vol. 1, pp. 58–62, Jan. 1977.

[2] S. S. Saad, J. B. Davies, and O. J. Davies, "Computer analysis of gradually tapered waveguide with arbitrary cross-sections," *IEEE Trans. Microwave Theory Tech.*, vol. MTT-25, pp. 437–440, May 1977.

[3] H. Flugel and E. Kuhn, "Computer-aided analysis and design of circular waveguide tapers," *IEEE Trans. Microwave Theory Tech.*, vol. 36, pp. 332–336, Feb. 1988.

[4] W. A. Huting and K. J. Webb, "Numerical solution of the continuous waveguide transition problem," *IEEE Trans. Microwave Theory Tech.*, vol. 37, pp. 1802–1808, Nov. 1989.
[5] W. A. Huting and K. J. Webb, "Numerical analysis of rectangular and circular waveguide tapers," *IEEE Trans. Magn.*, vol. 25, pp. 3095–3097, July 1989.
[6] G. Reiter, "Generalized telegraphist's equation for waveguides of varying cross-section," *Proc. Inst. Elec. Eng.*, vol. 106B, supplement 13, pp. 54–57, Sept. 1959.
[7] W. A. Huting, "Comparison of various techniques in the analysis of waveguide transitions," Johns Hopkins University Applied Physics Laboratory TG-draft, Laurel, MD, 1990.
[8] W. A. Huting, "Numerical analysis of tapered waveguide transitions," Ph.D. dissertation, University of Maryland, College Park, MD, Aug. 1989.
[9] L. Carin, K. J. Webb, and S. Weinreb, "Matched windows in circular waveguide," *IEEE Trans. Microwave Theory Tech.*, vol. 36, pp. 1359–1362, Sept. 1988.
[10] T. S. Chu and T. Itoh, "Generalized scattering matrix method for analysis of cascaded and offset microstrip step discontinuities," *IEEE Trans. Microwave Theory Tech.*, vol. MTT-34, pp. 280–284, Feb. 1986.
[11] G. R. P. Marie, "Mode transforming waveguide transition," U.S. Patent No. 2 859 412, Nov. 4, 1958.
[12] T. N. Anderson, "Low loss transmission using overmoded waveguide: A practical 1981 review of the state of the art," presented at IEEE AP/MTT-S Philadelphia Section Benjamin Franklin 1981 Symp. Advances in Antenna and Microwave Technology, Philadelphia, May 16, 1981.
[13] S. S. Saad, "Computer analysis and design of gradually tapered waveguide with arbitrary cross-sections," Ph.D. dissertation, University College, London, Oct. 1973.
[14] L. Solymar, "Spurious mode generation in nonuniform waveguide," *IRE Trans. Microwave Theory Tech.*, vol. MTT-7, pp. 379–383, July 1959.
[15] M. T. Menzel and H. K. Stokes, "User's guide for the POISSON/SUPERFISH group of codes," Los Alamos National Laboratory LA-UR-87-115, Los Alamos, NM, Jan. 1987.
[16] A. Konrad and P. P. Silvester, "Scalar finite-element package for two-dimensional field problems," *IEEE Trans. Microwave Theory Tech.*, vol. MTT-19, pp. 952–954, Dec. 1971.
[17] F. Sporleder and H.-G. Unger, *Waveguide Tapers, Transitions, and Couplers*. New York: Peter Peregrinus, 1979.
[18] R. H. Dicke, "General microwave circuit theorems," in *Principles of Microwave Circuits*, C. G. Montgomery, R. H. Dicke, and E. M. Purcell, Eds., New York: McGraw-Hill, 1948, pp. 130–161.
[19] N. Marcuvitz, *Waveguide Handbook*. New York: McGraw-Hill, 1951. Reprinted by Peter Peregrinus, 1986.
[20] H.-G. Unger, "Circular waveguide taper of improved design," *Bell Syst. Tech. J.*, vol. 37, pp. 899–912, July 1958.

✠

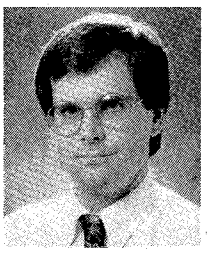

William A. Huting (S'80–M'84) was born in Ann Arbor, MI, on June 23, 1959. He received the B.S.E. degree in electrical engineering from Duke University in 1981, the M.S.E.E. degree from Georgia Tech in 1982, and the Ph.D. degree in electrical engineering from the University of Maryland in 1989.

Since 1984 he has been with The Johns Hopkins University Applied Physics Laboratory, where he has principally been involved with investigations of circular overmoded waveguides and tapered waveguide transitions.

✠

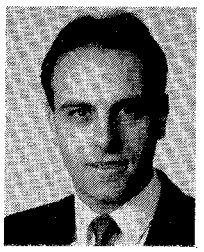

Kevin J. Webb (S'81–M'84) received the B.Eng. and M.Eng. degrees in communication and electronic engineering from the Royal Melbourne Institute of Technology, Australia, in 1978 and 1983, respectively, the M.S.E.E. degree from the University of California, Santa Barbara, in 1981, and the Ph.D. degree in electrical engineering from the University of Illinois, Urbana, in 1984.

From 1984 until 1989 he was an Assistant Professor in the Electrical Engineering Department at the University of Maryland, College Park. He is now an Associate Professor in the School of Electrical Engineering, Purdue University, West Lafayette, IN. His research interests include microwave and millimeter-wave integrated circuits, VLSI circuits, optoelectronics, and diffractive gratings.